# Ambiguity Function Analysis for Dual-Function Radar Communications Using PSK Signaling

Indu Priya Eedara*, Aboulnasr Hassanien†, Moeness G. Amin*, Brian D. Rigling†

*Centre for Advanced Communications, Villanova University, Villanova, PA, 19085, USA
E-mail: {ieedara; moeness.amin}@villanova.edu
†Department of Electrical Engineering, Wright State University, Dayton, OH 45435, USA
E-mail: {nasr.hassanien; brian.rigling}@wright.edu

***Abstract*—There is a presumed adverse effect on radar operation brought about from embedding communication signals in radar waveforms. Contrary to that presumption, we show in this paper that modulation of the radar pulse can indeed benefit both radar and communications in the dual system paradigm. This is shown by analyzing the impact of phase-shift keying (PSK) symbol embedding on the ambiguity function (AF) of a multiple-input multiple-output (MIMO) radar. Our analysis shows that the embedded PSK symbols yield reduction in the AF sidelobe peaks for a single pulse as well as for a series of radar pulses. To prove these results, we analyze the AF with and without the PSK symbol embedding. It is shown that the embedding of PSK symbols enable increasing the number of orthogonal transmit waveforms that can be used without increasing the sidelobe levels (SLL) of the corresponding AF.**

## I. Introduction

The increasing demands of the commercial wireless communications industry have created radio frequency (RF) spectrum congestion challenges, stirring much activities and strong interest in spectrum sharing [1]–[3]. Spectrum sharing research has been divided into two categories [4]: 1) the radar and communication systems coexist as separate systems that, in some way, respond/adapt to one another and 2) the two systems represent facets of the same multi-function RF system. The former is an interference mitigation problem that could employ dynamic spectral sensing and access, possibly combined with adaptive cancellation. The latter is considered a co-design approach, where the radar and communication systems use the same bandwidth. The underlying concept of the co-design provides uncontested shared bandwidth between wireless communication and radar systems.

In the co-design problem considered, the radar and the communication systems share the same resources, including bandwidth and without multiplexing [5]–[9]. As such, the same system is tasked with dual functionalities. When communications is treated as the secondary function to the primary radar function, the system is referred to as Dual-Function Radar-Communication (DFRC) [10]–[14]. Embedding of information into radar waveforms can be performed using different strategies [12], most notably those based on multiple-input multiple-output (MIMO) radar configurations.

In this paper, we show that using certain radar waveforms and configurations, communication embedding benefits dual system functionalities. We adopt the signaling scheme employed in [15] where information embedding is performed using frequency-hopping (FH) waveforms in MIMO radar. We examine the impact of embedding Phase Shift Keying (PSK) communication symbols on the MIMO radar functionality. The ambiguity function (AF) of FH-based MIMO radar typically exhibits large sidelobes due to the re-use of the FH coefficients within the same pulse. This limits the number of orthogonal FH waveforms that can be synthesized. It is shown that PSK communication symbol embedding in FH-based MIMO radar functionality reduces the sidelobe level (SLL) of the AF. As a result, a large number of orthogonal FH waveforms can be synthesized via increasing the rate of FH coefficient recurrence while reducing the AF SLL. Therefore, the achievable communication data rate can be increased without altering or compromising the MIMO radar functionality.

The paper is organized as follows. Signal models are given in Sec. II. PSK symbol embedding is presented in Sec. III. The AF is derived and analyzed in Sec. IV. Simulation results are given in Sec. V, and Conclusions are drawn in Sec. VI.

## II. MIMO Radar Signal Model

Consider a DFRC system equipped with a co-located transmit array of $M_t$ isotropic antennas arranged in a linear shape. The DFRC transmit platform performs the radar and communication functions simultaneously by transmitting $M_t$ orthogonal waveforms while embedding information into the radar emission. The MIMO radar receive array comprises $M_r$ co-located antennas arranged in an arbitrary linear shape. We assume that both the transmit and receive arrays closely spaced such that a target in the far-field appears in the same spatial direction with respect to both arrays. Let $\phi_m(t), m = 1 \dots M_t$, be $M_t$ waveforms which satisfy the orthogonality condition

$$\int_{T_p} \phi_m(t)\phi^*_{m'}(t+\tau)e^{j2\pi\nu t}dt = \begin{cases} \delta(\tau)\delta(\nu), \ m = m', \\ 0, \ \text{otherwise} \end{cases} \quad (1)$$

The work by InduPriya Eedara and Moeness Amin is supported by the National Science Foundation, grant no. AST-1547426

where $t$ is the fast-time index, $T_p$ is the pulse duration, $(\cdot)^*$ denotes the conjugate of a complex number, $\tau$ and $\nu$ denote time delay and Doppler shift, respectively, and $\delta(\cdot)$ is the Kronecker delta function. It is worth noting that, in practice, it is difficult to synthesize waveforms which satisfy the ideal orthogonality condition (1). However, practical waveforms can be efficiently synthesized (see [16]; and references therein).

### A. Orthogonal Frequency-Hopping Waveforms

From a MIMO radar perspective, practical waveforms should enable achieving high transmit power efficiency and high radar and Doppler resolution properties. In this respect, the use of orthogonal FH waveforms for MIMO radar has been reported in a number of papers [17]–[19]. FH waveforms are inherently power efficient due to the constant-modulus property. In addition, they are simple to generate and immune to interference. The $m^{\text{th}}$ FH waveform can be expressed as

$$\phi_m(t) = \sum_{q=1}^{Q} e^{j2\pi c_{m,q}\Delta_f t} u(t - q\Delta_t) \tag{2}$$

where $c_{m,q},\ m = 1, \ldots, M_t,\ q = 1, \ldots, Q$ denote the FH coefficients, $Q$ is the FH code length, $\Delta_f$ and $\Delta_t$ are the frequency step and the sub-pulse duration respectively, and

$$u(t) \triangleq \begin{cases} 1, & 0 < t < \Delta_t, \\ 0, & \text{otherwise}. \end{cases} \tag{3}$$

is a rectangular pulse of duration $\Delta_t$. Equation (2) implies that each FH waveform contains $Q$ sub-pulses, i.e., the pulse duration $T_p = Q\Delta_t$. It is also assumed that $\Delta_t\Delta_f$ is an integer.

Let $B$ be the bandwidth assigned to the DFRC system. To insure that the spectral contents of the orthogonal FH waveforms are confined to the available bandwidth, the FH code should be selected from the set of integers $\{0, 1, \ldots, K-1\}$. Then, the effective bandwidth of the pulse can be approximated as

$$B_{\text{eff}} \approx (K-1)\Delta_f + \frac{1}{\Delta_t}. \tag{4}$$

We assume that the value of $K$ is properly selected such that the condition $B_{\text{eff}} \leq B$ is satisfied. The time-bandwidth product of the DFRC system is given as

$$BT_p = \left((K-1)\Delta_f + \frac{1}{\Delta_t}\right) Q\Delta_t = KQ. \tag{5}$$

### B. MIMO Radar Receive Signal Model

Assuming that the signals reflected by $L$ targets impinge on the MIMO radar receiver from directions $\theta_\ell,\ \ell = 1, \ldots, L$. We consider the signal model given in [20] to express the $M_r \times 1$ complex-valued vector of the received baseband signals, that is

$$\mathbf{x}(t,n) = \sum_{\ell=1}^{L} \beta_\ell(n) \left[\mathbf{a}^T(\theta_\ell)\, \boldsymbol{\phi}(t)\right] \mathbf{b}(\theta_\ell) + \mathbf{z}(t,n), \tag{6}$$

where $n$ denotes the slow-time index, i.e., pulse number, $\beta_\ell(n)$ is the reflection coefficient associated with the $\ell^{\text{th}}$ target during the $n^{\text{th}}$ pulse, $\theta_\ell$ is the spatial angle of the $\ell^{\text{th}}$ target, $\mathbf{a}(\theta_\ell)$ and $\mathbf{b}(\theta_\ell)$ are the steering vectors of the transmit and receive arrays towards the direction $\theta_\ell$, respectively, $(\cdot)^T$ stands for the transpose, $\boldsymbol{\phi}(t) \triangleq [\phi_1(t), \ldots, \phi_{M_t}(t)]^T$ is the $M_t \times 1$ complex vector of orthogonal waveforms, and $\mathbf{z}(t,n)$ is an $M_r \times 1$ vector of zero-mean white Gaussian noise. In (6), the reflection coefficients $\beta_\ell(n),\ \ell = 1, \ldots, L$, are assumed to obey the Swerling II target model. Matched filtering (6) to the transmitted orthogonal waveforms yields the $M_tM_r \times 1$ extended vector of virtual data, that is

$$\begin{aligned} \mathbf{y}(n) &= \operatorname{vec}\left(\int_{T_p} \mathbf{x}(t,n)\, \boldsymbol{\phi}^H(t)\, dt\right) \\ &= \sum_{\ell=1}^{L} \beta_\ell(n) \left[\mathbf{a}(\theta_\ell) \otimes \mathbf{b}(\theta_\ell)\right] + \tilde{\mathbf{z}}(n), \end{aligned} \tag{7}$$

where $\operatorname{vec}(\cdot)$ denotes the vectorization operator that stacks the columns of a matrix into one long column vector, $\otimes$ denotes the Kronecker product, $(\cdot)^H$ stands for the Hermitian transpose, $\tilde{\mathbf{z}}(n)$ is $M_tM_r \times 1$ vector of additive noise at the output of the matched-filters with zero-mean and co-variance $\sigma_z^2 \mathbf{I}_{M_tM_r}$, and $\mathbf{I}_M$ is the identity matrix of size $M \times M$.

## III. PSK Symbol Embedding

This section provides a concise overview of PSK symbol embedding into the emission of MIMO radar using FH waveforms. For more information on this PSK signaling scheme, the reader is referred to [15].

Let $\{\Omega_{m,q}^{(n)} \in \mathbb{D}_{\text{PSK}},\ m = 1, \ldots, M_t,\ q = 1, \ldots, Q$ be a set of PSK symbols that need to be embedded into the MIMO radar emission during the $n^{\text{th}}$ pulse, where $\mathbb{D}_{\text{PSK}} = \left\{0, \frac{2\pi}{J}, \ldots, \frac{(J-1)2\pi}{J}\right\}$ is a PSK dictionary and $J$ is the dictionary size. Each PSK symbol represents $N_{\text{bit}} = \log_2 J$ bits. Then, the PSK-modulated FH waveforms are defined as

$$\psi_m(t,n) = \sum_{q=1}^{Q} e^{j\Omega_{(m,q)}^{(n)}} h_{m,q}(t) u(t - q\Delta t - nT_0), \tag{8}$$

where $h_{m,q}(t) \triangleq e^{j2\pi c_{m,q}\Delta_f t}$ is the FH signal associated with the $m^{\text{th}}$ antenna during the $n^{\text{th}}$ sub-pulse and $T_0$ is the pulse repetition interval.

Consider a single-antenna communication receiver located at in the spatial direction $\theta_c$ with respect to the MIMO radar. Then, the signal at the output of the communication receiver can be expressed as

$$r(t,n) = \alpha_{\text{ch}} \mathbf{a}^T(\theta_c) \boldsymbol{\psi}(t,n) + w(t,n), \tag{9}$$

where $\alpha_{\text{ch}}$ is the channel coefficient which summarizes the propagation environment between the MIMO radar transmit array and the communication receiver, $\boldsymbol{\psi}(t,n) \triangleq [\psi_1(t,n), \ldots, \psi_{M_t}(t,n)]^T$ is the vector of PSK modulated waveforms, and $w(t,n)$ represents the additive white Gaussian noise with zero mean and variance $\sigma_w^2$.

Assume that time and phase synchronization between the

MIMO radar and the communication receiver is achieved. Then, matched filtering $r(t,n)$ to the FH sub-pulses yields

$$\begin{aligned} y_{m,q}(n) &= \int_{\Delta_t} r(t,n) h^*_{m,q}(t) u(t - q\Delta_t - nT_0) dt \\ &= \alpha_{\mathrm{ch}} e^{j\left(\Omega^{(n)}_{(m,q)} - 2\pi d_m \sin\theta_c\right)} + w_{m,q}(n), \end{aligned} \qquad (10)$$

where $\mathbf{a}_{[m]} \triangleq e^{-j2\pi d_m \sin\theta_c}$ stands for the $m^{\text{th}}$ entry of $\mathbf{a}(\theta_c)$, $d_m$ is the displacement between the first and the $m^{\text{th}}$ elements of the transmit array measured in wavelength, and $w_{m,q}(n) \triangleq \int_0^{\Delta_t} w(t,n) h^*_{m,q}(t) u(t - \Delta_t - nT_0) dt$ is the additive noise term at the output of the $(m,q)^{\text{th}}$ matched filter with zero mean and variance $\sigma_w^2$. Then, the embedded PSK symbols can be estimated as

$$\hat{\Omega}^{(n)}_{m,q} = \angle\big(y_{m,q}(n)\big) - \varphi_{\mathrm{ch}} + 2\pi d_m \sin\theta_c, \qquad (11)$$

where $\angle(\cdot)$ stands for the angle of a complex number and $\varphi_{\mathrm{ch}} \triangleq \angle(\alpha_{\mathrm{ch}})$ is the phase of the channel coefficient.

## IV. Ambiguity Function Analysis

This section provides analysis of the AF of PSK-based information embedding into the FH MIMO radar waveforms. We consider the case of a single pulse as well as the case of a pulse train. It is shown that the embedding of PSK symbols enables reducing the SLL of the AF as compared to the case of MIMO radar without symbol embedding.

The selection of the FH code matrix to optimize the radar operation has been recently reported in [19]. However, for DFRC system using FH waveforms, an additional constraint on the orthogonality between the FH waveforms from sub-pulse to another is mandated by the communication function of the system. Specifically, the condition

$$c_{m,q} \neq c_{m',q}, \qquad \forall q, m \neq m' \qquad (12)$$

should be satisfied while selecting the FH code to enable symbol detection at the communication receiver. In this respect, we generate the FH code for each sub-pulse using an iterative random frequency generation until condition (12) is satisfied.

### A. Ambiguity Function for a Single Radar Pulse

Without loss of generality, we consider the case of a DFRC system with uniform linear arrays. The inter-element spacings associated with the transmit and receive arrays are denoted as $d_T$ and $d_R$, respectively. The spatial frequency of a hypothetical target located in direction $\theta$ is defined as $f = 2\pi d_R sin(\theta/\lambda)$, where $\lambda$ is the carrier wavelength. Adopting the AF definition of the MIMO radar from [17], the AF expression for the MIMO radar can be written as

$$\Big|\chi(\tau,\nu,f,f')\Big| \triangleq \left|\sum_{m=1}^{M_t}\sum_{m'=1}^{M_t} \chi_{m,m'}(\tau,\nu) e^{j2\pi(fm - f'm')\gamma}\right|, \qquad (13)$$

where, $\tau, \nu, f, f'$ denote time delay, Doppler shift, spatial frequency, and spatial frequency shift, respectively, $\gamma \triangleq d_T/d_R$, and

$$\chi_{m,m',q,q'}(\tau,\nu) \triangleq \int_0^{T_p} \phi_m(t)\phi^*_{m'}(t+\tau) e^{j2\pi\nu t} dt \qquad (14)$$

is the cross-ambiguity function. The AF for MIMO radar using FH waveforms is given by

$$\Big|\chi_{\mathrm{radar}}(\tau,\nu,f,f')\Big| = \Big|\sum_{m=1}^{M_t}\sum_{m'=1}^{M_t}\sum_{q=1}^{Q}\sum_{q'=1}^{Q} \chi^{(\Delta_t)}_{m,m',q,q'}(\tau,\nu) e^{j2\pi(fm - f'm')\gamma}\Big|, \qquad (15)$$

where the cross AF of two sub-pulses is defined as

$$\chi^{(\Delta_t)}_{m,m',q,q'}(\tau,\nu) \quad = \quad \chi^{rect}(\tau_1,\nu_1) e^{j2\pi c_{m',q'}\Delta_f \tau}, \qquad (16)$$

$$\begin{aligned} \chi^{rect}(\tau_1,\nu_1) &\triangleq \int_0^{\Delta_t} u(t)u(t+\tau) e^{(j2\pi\nu t)} dt, \quad |\tau| \leq \Delta_t \\ &= \frac{\Delta_t - |\tau|}{\Delta_t} \mathrm{sinc}\big(\nu(\Delta_t - |\tau|)\big).e^{j\pi\nu(\Delta_t - |\tau|)}. \end{aligned} \qquad (17)$$

In (16), $\nu_1 \triangleq (c_{m,q} - c_{m',q'})\Delta_f + \nu$ and $\tau_1 \triangleq (\tau - (q'\Delta_t - q\Delta_t))$ are auxiliary Doppler-shift and time-delay, respectively.

For the DFRC system, the AF expression with PSK symbol embedding is given as

$$|\chi_{\mathrm{DFRC}}(\tau,\nu,f,f')| = \Big|\sum_{m=1}^{M_t}\sum_{m'=1}^{M_t}\sum_{q=1}^{Q}\sum_{q'=1}^{Q} \chi^{(\Delta_t)}_{m,m',q,q'}(\tau,\nu) e^{j(\Omega_{(m,q)} - \Omega_{(m',q')})}.e^{j2\pi(fm - f'm')\gamma}\Big|. \qquad (18)$$

By using the guidelines provided in [21] and the triangle inequality, bounds on the maximum SLL for the DFRC system design is given by the following condition

$$|\chi_{\mathrm{DFRC}}(\tau,\nu,f,f')|_{\max} \leq \sum_{m=1}^{M_t}\sum_{m'=1}^{M_t}\sum_{q=1}^{Q}\sum_{q'=1}^{Q} \Big|e^{j\Omega_{(m,q)}} e^{-j\Omega_{(m',q')}}\Big| \cdot \Big|\chi^{(\Delta_t)}_{m,m',q,q'}(\tau,\nu).e^{j2\pi(fm - f'm')\gamma}\Big|, \qquad (19)$$

where $|\cdot|_{\max}$ denotes the maximum value of the magnitude of the argument. Using the fact that $\Big|e^{j(\Omega_{(m,q)} - \Omega_{(m',q')})}\Big| = 1$ and making use of (15) and (19), it is straightforward to show that,

$$|\chi_{\mathrm{DFRC}}(\tau,\nu,f,f')|_{\max} \leq |\chi_{\mathrm{radar}}(\tau,\nu,f,f')|_{\max}. \qquad (20)$$

Equation (20) shows that the highest SLL of the DFRC AF is less than or equal to the highest SLL of the MIMO radar AF. In this respect, few comments are in order.

*Remark 1*: The number of FH's within a single radar pulse is $M_t Q$. Assuming that each FH coefficient is used with equal probability, the rate of occurrence of each coefficient within the same pulse is $M_t Q/K$. In addition, the maximum number of FH waveforms that can be utilized without violating the orthogonality condition (12) is $M_t = K$. In this case, the number of FH sub-pulses within one radar pulse is $KQ$ which means that, on average, each of the $K$ FH coefficients occurs $Q$ times within the same pulse.

*Remark 2*: The MIMO radar AF (15) exhibits spike-like SLL at the delay instances (assuming zero Doppler shift) given by $|\tau| = i\Delta_t,\ i = 1, \ldots, Q-1$. This can be attributed to the fact that, at these delay instances, every pair of sub-pulses that are shifted from one another by time separation $(q-q')\Delta_t = i\Delta_t,\ q, q' = 1, \dots, Q$ becomes fully overlapping. In addition, the cross AF of each pair of fully overlapped sub-pulses, e.g., (16), has a maximum value of the peak of the $\mathrm{sinc}$ function in (17). Therefore, increasing the re-occurrence of the FH coefficients within the same pulse results in higher SLLs of the MIMO radar AF.

*Remark 3*: The SLLs of the AF of the DFRC system given in (18) depends on the the embedded PSK symbols $\Omega_{(m,q)},\ \Omega_{(m',q')}$. Since the PSK symbols are inherently random, the summation in (18) results in reduced SLLs at delays $|\tau| = i\Delta_t,\ i = 1, \dots, Q-1$ (assuming zero Doppler shift). Theoretically, considering that each PSK symbol represents a random variable and taking the ensemble of (18) yields zero SLL at delays $|\tau| = i\Delta_t,\ i = 1, \dots, Q-1$. This implies that performing the summation in (18) over a sufficiently large number of sub-pulses results in nearly zero SLLs of the DFRC AF at delays $|\tau| = i\Delta_t,\ i = 1, \dots, Q-1$. To demonstrate this property, we analyze the MIMO radar and DFRC AFs for a train of pulses in the next subsection.

### B. Ambiguity Function for a Train of Pulses

Here, we discuss the AF for a series of pulses of the presented DFRC system.
The pulse train of FH pulses can be represented as

$$\phi_{m,n}(t) = \sum_{n=0}^{N_p-1} \sum_{q=1}^{Q} h_{m,q}(t) u(t - q\Delta_t - nT_0), \tag{21}$$

where, $N_p$ is the number of pulses and $n = 0, \dots, N_p - 1$. The equation of the FH waveforms after embedding information symbols into $n^{\text{th}}$ pulse is given by

$$\psi_m(t, n) = \sum_{n=0}^{N_p-1} \sum_{q=1}^{Q} e^{j\Omega_{(m,q)}^{(n)}} h_{m,q}(t) u(t - q\Delta_t - nT_0), \tag{22}$$

The AF for MIMO radar using FH waveforms for $N_p$ pulses is given by

$$|\chi_{\text{radar}}^{(\text{PT})}(\tau, \nu, f, f')| = \Bigg| \sum_{n=0}^{N_p-1} \sum_{n'=0}^{N_p-1} \sum_{m=1}^{M_t} \sum_{m'=1}^{M_t} \sum_{q=1}^{Q} \sum_{q'=1}^{Q} \chi_{m,m',q,q'}^{(\Delta_t)}(\tau - (n'-n)T_0, \nu) e^{j2\pi\nu n T_0} \Bigg|. \tag{23}$$

To analyze the dual-function embedded communication radar waveform of $N_p$ pulses, we compute the AF of the designed waveform (22) as

$$|\chi_{\text{DFRC}}^{(\text{PT})}(\tau, \nu, f, f')| = \Bigg| \sum_{n=0}^{N_p-1} \sum_{n'=0}^{N_p-1} \sum_{m=1}^{M_t} \sum_{m'=1}^{M_t} \sum_{q=1}^{Q} \sum_{q'=1}^{Q} e^{j(\Omega_{(m,q)}^{(n)} - \Omega_{(m',q')}^{(n')})} \chi_{m,m',q,q'}^{(\Delta_t)}(\tau - (n'-n)T_0, \nu) e^{j2\pi\nu n T_0} \Bigg|. \tag{24}$$

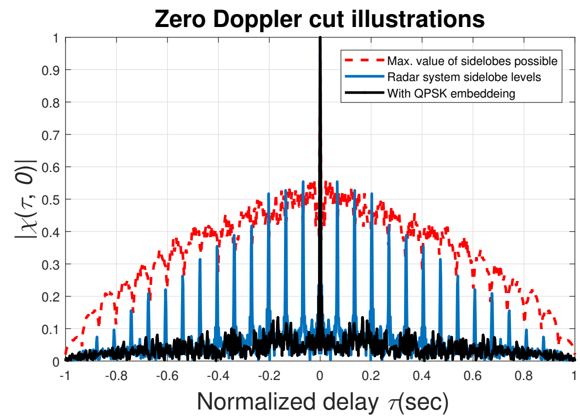


Fig. 1: Zero Doppler for single pulsed MIMO radar with and without PSK symbols embedded in FH waveforms

Equation (24) shows that, if the number of pulses in the summation of AF is large enough, the SLLs will be reduced and the AF will be close to the thumbtack shape.

## V. Simulation Results

In this section, we present simulation results for the radar waveforms with one pulse and series of pulses with and without the communication symbols embedded into the FH waveforms.

We consider a MIMO radar system operating at X-band with carrier frequency $f_c = 8.2$ GHz and bandwidth 100 MHz. The sampling frequency is taken as the Nyquist rate, i.e., $f_s = 2 \times 10^8$ sample/sec. The PRI is $T_0 = 10\mu s$, i.e., the PRF is 100 KHz. The transmit array is considered to be a ULA comprising $M_t = 10$ omni-directional transmit antennas spaced half a wavelength apart. We generate a set of 16 FH waveforms. The parameter $K = 16$ is chosen such that the FH step is $\Delta_f = 6$ MHz. The FH code length $Q = 15$ is assumed, and the FH interval duration $\Delta_t = 0.167\mu s$ is used. The $10 \times 15$ FH code is generated randomly from the set $\{1, 2, \dots, K\}$, where $K = 16$ is used.We used QPSK signal embedding to study the effect of PSK symbols on the AF.

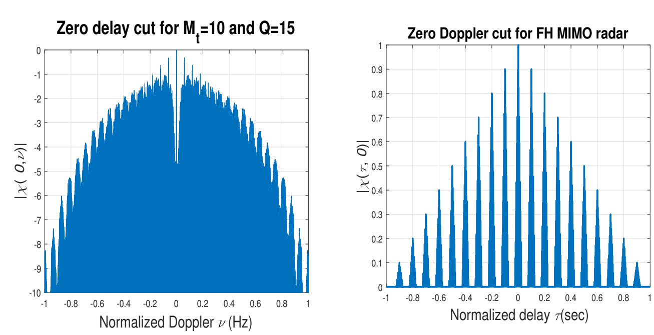


(a) Zero Delay cut

(b) Zero Doppler cut

Fig. 2: Zero Delay and Doppler cuts for MIMO radar with 10 pulses using FH waveforms

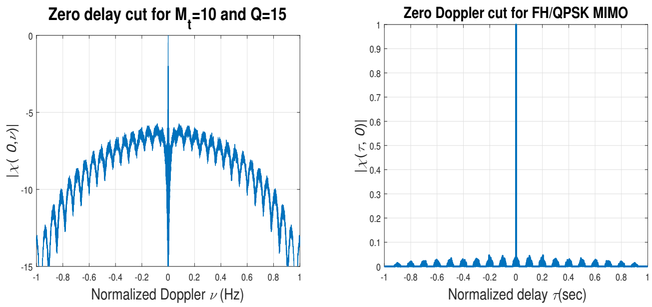


(a) Zero Delay cut (b) Zero Doppler cut

Fig. 3: Zero Delay and Doppler cuts for MIMO radar with 10 pulses with QPSK embedding into FH waveforms.

From Fig. 1, we can observe that the auto-correlation function (ACF) of the MIMO FH waveforms with and without embedding PSK symbols does not exceed the value of the maximum value defined by condition (20). Further, it is evident that the PSK information embedding considerably reduces the SLLs of the AF.

Fig. 2 and Fig. 3, we present the simulation results for the case of a series of MIMO radar pulses with and without information embedding. Again, we observe from these figures that embedding QPSK symbols into each hop of the radar pulses significantly reduces the sidelobe peaks of the AF.

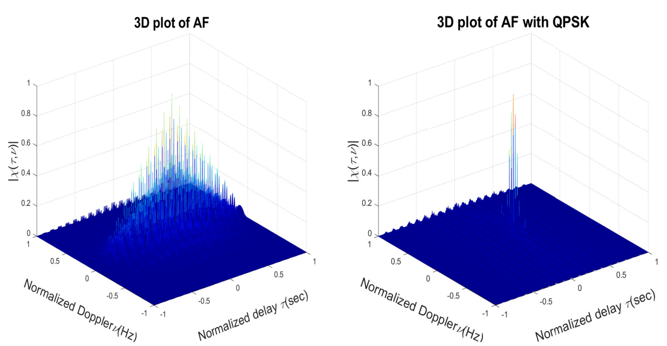


(a) 3D plot of MIMO AF using FH waveforms (b) 3D plot of AF with QPSK embedding

Fig. 4: 3D plots of AF with and without communication symbols embedded into FH MIMO radar waveforms

The 3D plots of the AF in Fig. 4a and Fig. 4b clearly show the reduction in the sidelobe peaks along both delay and Doppler with and without PSK symbol embedding.

## VI. Conclusion

In this paper, a dual-functionality system for co-design of radar and communication operation was considered. For each transmit antenna, a PSK communication symbol is embedded during each FH interval. The dependency of the ambiguity function on the embedded PSK communication symbols for both cases of a single pulse and a series of pulses was analyzed. Most importantly, it was shown that the associated maximum sidelobe levels can never exceed the maximum level represented by the conventional MIMO radar system using FH waveforms. In essence, embedding the PSK symbols into the MIMO radar pulses using FH waveforms reduces the sidelobe levels of the ambiguity function of the underlying DFRC system. The same system can achieve a data rate ($R = B \cdot M_t \cdot Q \cdot \mathrm{PRF}.\log_2(J)$) in the range of several hundreds of Mbps.

## References

[1] H. Griffiths, S. Blunt, L. Cohen, and L. Savy, "Challenge problems in spectrum engineering and waveform diversity," in *Proc. IEEE Radar Conf.*, April 2013, pp. 1–5.

[2] C. Baylis, M. Fellows, L. Cohen, and R. J. M. II, "Solving the spectrum crisis: Intelligent, reconfigurable microwave transmitter amplifiers for cognitive radar," *IEEE Microwave Magazine*, vol. 15, no. 5, pp. 94–107, July 2014.

[3] B. Li, H. Kumar, and A. P. Petropulu, "A joint design approach for spectrum sharing between radar and communication systems," in *2016 IEEE International Conference on Acoustics, Speech and Signal Processing (ICASSP)*, March 2016, pp. 3306–3310.

[4] P. M. McCormick, S. D. Blunt, and J. G. Metcalf, "Simultaneous radar and communications emissions from a common aperture, part I: Theory," in *Proc. IEEE Radar Conf.*, May 2017, pp. 1685–1690.

[5] A. Khawar, A. Abdelhadi, and C. Clancy, "Target detection performance of spectrum sharing MIMO radars," *IEEE Sensors Journal*, vol. 15, no. 9, pp. 4928–4940, 2015.

[6] L. Wang, J. McGeehan, C. Williams, and A. Doufexi, "Application of cooperative sensing in radar–communications coexistence," *IET communications*, vol. 2, no. 6, pp. 856–868, 2008.

[7] K.-W. Huang, M. Bica, U. Mitra, and V. Koivunen, "Radar waveform design in spectrum sharing environment: Coexistence and cognition," in *Proc. IEEE Radar Conf.*, May 2015, pp. 1698–1703.

[8] Y. L. Sit, C. Sturm, L. Reichardt, T. Zwick, and W. Wiesbeck, "The OFDM joint radar-communication system: An overview," in *Int. Conf. Advances in Satellite and Space Communications*, 2011, pp. 69–74.

[9] S. Ji, H. Chen, Q. Hu, Y. Pan, and H. Shao, "A dual-function radar-communication system using FDA," in *2018 IEEE Radar Conference (RadarConf18)*, April 2018, pp. 0224–0229.

[10] S. D. Blunt, M. R. Cook, and J. Stiles, "Embedding information into radar emissions via waveform implementation," in *Int. Waveform Diversity and Design Conf.* IEEE, 2010, pp. 195–199.

[11] J. Euziere, R. Guinvarc'h, M. Lesturgie, B. Uguen, and R. Gillard, "Dual function radar communication time-modulated array," in *Proc. IEEE Int. Radar Conf.*, 2014, pp. 1–4.

[12] A. Hassanien, M. G. Amin, Y. D. Zhang, and F. Ahmad, "Dual-function radar-communications using phase-rotational invariance," in *European Signal Processing Conf.*, Aug 2015, pp. 1346–1350.

[13] ——, "Phase-modulation based dual-function radar-communications," *IET Radar, Sonar Navigation*, vol. 10, no. 8, pp. 1411–1421, 2016.

[14] ——, "Signaling strategies for dual-function radar communications: An overview," *IEEE Aerospace and Electronic Systems Magazine*, vol. 31, no. 10, pp. 36–45, October 2016.

[15] A. Hassanien, B. Himed, and B. D. Rigling, "A dual-function MIMO radar-communications system using frequency-hopping waveforms," in *Proc. IEEE Radar Conf.*, May 2017, pp. 1721–1725.

[16] S. D. Blunt and E. L. Mokole, "Overview of radar waveform diversity," *IEEE Aerospace and Electronic Systems Magazine*, vol. 31, no. 11, pp. 2–42, November 2016.

[17] C. Y. Chen and P. P. Vaidyanathan, "MIMO radar ambiguity properties and optimization using frequency-hopping waveforms," *IEEE Transactions on Signal Processing*, vol. 56, no. 12, pp. 5926–5936, Dec 2008.

[18] G. V. K. Sharma, P. Srihari, and K. R. Rajeswari, "MIMO radar ambiguity analysis of frequency hopping pulse waveforms," in *2014 IEEE Radar Conference*, May 2014, pp. 1241–1246.

[19] K. Han and A. Nehorai, "Jointly optimal design for MIMO radar frequency-hopping waveforms using game theory," *IEEE Transactions on Aerospace and Electronic Systems*, vol. 52, no. 2, pp. 809–820, April 2016.

[20] J. Li and P. Stoica, *MIMO radar signal processing*. John Wiley & Sons, 2008.

[21] Y. I. Abramovich and G. J. Frazer, "Bounds on the volume and height distributions for the MIMO radar ambiguity function," *IEEE Signal Processing Letters*, vol. 15, pp. 505–508, 2008.